PHYSICAL REVIEW D **78,** 104017 (2008)

Stability of higher dimensional Reissner-Nordström-anti-de Sitter black holes

R. A. Konoplya*
Department of Physics, Kyoto University, Kyoto 606-8501, Japan

A. Zhidenko†
Instituto de Física, Universidade de São Paulo C.P. 66318, 05315-970, São Paulo-SP, Brazil
(Received 11 September 2008; published 18 November 2008)

We investigate stability of the D-dimensional Reissner-Nordström-anti-de Sitter metrics as solutions of the Einstein-Maxwell equations. We have shown that asymptotically anti-de Sitter (AdS) black holes are dynamically stable for all values of charge and anti-de Sitter radius in $D = 5, 6 \ldots 11$ dimensional space-times. This does not contradict dynamical instability of RNAdS black holes found by Gubser in $\mathcal{N} = 8$ gauged supergravity, because the latter instability comes from the tachyon mode of the scalar field, coupled to the system. Asymptotically AdS black holes are known to be thermodynamically unstable for some region of parameters, yet, as we have shown here, they are stable against gravitational perturbations.

DOI: 10.1103/PhysRevD.78.104017 PACS numbers: 04.30.Nk

I. INTRODUCTION

Nowadays, brane world theories and string theory imply existence of extra dimensions in nature [1]. This induced great interest to higher dimensional black holes, in particular, to such features as perturbations, dynamical and thermodynamical stability, particles and fields behavior, and Hawking radiation around these black holes. Unlike the four-dimensional case, higher dimensional space-times admit plenty of ''black'' solutions: black holes, black strings and branes, black rings, and Saturns. Stability of these solutions may be criteria of their existence. The stability analysis usually requires one to transform the perturbed Einstein equation to the wavelike form, what was done yet in 1957 by Regge and Wheeler for $D = 4$ black holes, and only in 2003 for a general number of space-time dimensions [2]. Then, the stability of D-dimensional Schwarzschild black holes was proved in [3] and of Schwarzschild-de Sitter black holes in [4]. Recently the stability of Kaluza-Klein black holes with squashed horizons was shown in [5,6]. Unlike Kaluza-Klein black holes, black strings and branes become unstable for perturbations with wavelength, which is larger than some threshold value (Gregory-Laflamme instability [7]). In [8] it was shown that the instability threshold point corresponds to some dominating static solution of the wave equation. The neutral D-dimensional black holes in Gauss-Bonnet theory are unstable only for $D = 5, 6$ and for small values of Gauss-Bonnet coupling [9,10]. The instability in the Gauss-Bonnet theory is qualitatively different from a black string instability: the black string instability is an example of instability, developed at the lowest multipoles, therefore with a static solution dominance at the threshold point. The instability in the Gauss-Bonnet theory is developed at large multipoles, so that the growing mode dominates after a long period of damped quasinormal oscillations [10].

The stability of the higher dimensional black holes is important also for the growing interest to the quasinormal modes of the standard model fields in higher dimensional theories [11]. Indeed, only stable black holes can be considered as a background on which test fields propagate. In this context, a gravitational instability of Reissner-Nordström-de Sitter black holes was found, when both charge and the Lambda term are large enough [12].

Higher dimensional black holes in asymptotically anti-de Sitter (AdS) space-times have been in the focus of string theorists in recent years, because of their role in the AdS/CFT correspondence. A large asymptotically anti-de Sitter black hole corresponds to a thermal state in the dual conformal field theory, where the Hawking temperature of the black hole is the temperature in the dual field theory [13]. The perturbations of AdS black holes have been extensively studied during the recent decade [14]. Nevertheless, it was not known until the present study if D-dimensional asymptotically AdS black holes are dynamically stable as solutions of D-dimensional Einstein-Maxwell equations. The stability of $D = 4$ and $D = 5$ Reissner-Nordström-AdS black holes was studied by Gubser and Mitra in the $\mathcal{N} = 8$ gauged supergravity theory [15,16], i.e. a theory with the Maxwell and scalar matter fields coupled to the electromagnetic field. There it was shown that the highly charged black holes are unstable and the parameter region of instability increases for larger black holes, i.e. for black holes, which radius is much larger than the anti-de Sitter radius. Yet that instability evidently came from the tachyonic mode of the scalar field. Thus the question remains if there is an instability of Reissner-Nordström-anti-de Sitter black holes within the ordinary Einstein-Maxwell theory. Our main aim here is to answer this question, keeping in mind such an important

*konoplya_roma@yahoo.com
†zhidenko@fma.if.usp.br

feature of black holes as thermodynamic (in)stability. Thus, according to hypothesis of Gubser and Mitra in [15,16], there may be a correlation between thermodynamic and dynamic (gravitational) (in)stabilities of black holes, because it was found that the parametric region of thermodynamic and dynamic (in)stabilities, although they do not coincide, differ from each other only slightly for the $\mathcal{N} = 8$ gauged supergravity. Another possible correlation could give the thermodynamic instability of small AdS black holes, which happens with a phase transition, called the Hawking-Page transition [17]. One of the thermodynamically preferred final states, after the transition, might be a pure AdS space-time [17].

The thermodynamic instability of black holes takes place also for ordinary Einstein-Maxwell-AdS black holes [18] for some values of black hole parameters. The second order phase transition occurs at the instability point [18]. If we expect some correlations between thermodynamic and dynamic instabilities to these cases, we should expect gravitational instability of D-dimensional charged black holes in AdS space-times within the standard Einstein-Maxwell theory. In this paper, we shall show that this is not the case of the pure RNAdS black holes, which are stable against gravitational perturbations for $D = 5, 6 \ldots 11$, where D is the number of space-time dimensions.

The paper is organized as follows: Section II introduces the basic formula for the background metric and for perturbation equations reduced to a wavelike form. Section III reviews the numerical method, which we used for stability analysis. Sections IV and V consider the obtained results for Reissner-Nordström-anti-de Sitter black holes.

II. BASIC FORMULAS

The metric of the $D = d + 2$-dimensional Reissner-Nordström-(anti)-de Sitter black holes is given by the line element

$$ds^2 = f(r)dt^2 - \frac{dr^2}{f(r)} - r^2 d\Omega_d, \tag{1}$$

where $d\Omega_d$ is the line element on a unit d sphere, and

$$f(r) = 1 - X + Z - Y, \qquad X = \frac{2M}{r^{d-1}}, \qquad Y = \frac{2\Lambda r^2}{d(d+1)}, \qquad Z = \frac{Q^2}{r^{2d-2}}. \tag{2}$$

Here M is the mass parameter of the black hole, Q is its charge, and the Λ term coincides with a cosmological constant, when positive, and is related to the anti-de Sitter radius, when negative, in the following way:

$$\frac{2\Lambda}{d(d+1)} = -\frac{1}{R^2} = -1.$$

The general perturbations of the Einstein-Maxwell equations

$$g_{\mu\nu} = g^0_{\mu\nu} + \delta g_{\mu\nu}, \tag{3}$$

$$\delta R_{\mu\nu} = \kappa\delta\left(T_{\mu\nu} - \frac{1}{D-2} T g_{\mu\nu}\right) + \frac{2\Lambda}{D-2}\delta g_{\mu\nu}, \tag{4}$$

after using the gauge freedom, and separating the angular variables can be reduced to a number of wavelike equations [2] for three types of gravitational perturbations, according to the symmetry of the rotation group: scalar, vector, and tensor. In four dimensions, the scalar type of gravitational perturbations is called polar, the vector type is called axial. The tensor type of gravitational perturbations is usually pure gauge in $D = 4$ black hole space-times. For $D = 4$ Reissner-Nordström-(anti)-de Sitter black holes, axial and polar types of perturbations are isospectral, so that for stability analysis it is enough to analyze only one type of perturbations. For $D > 4$, the isospectrality is broken, so that one needs to check all three kinds of perturbations. The vector and tensor types of gravitational perturbations were shown to be stable [2] for all D, with the help of the so-called S-deformation technique. Therefore we shall consider here only the scalar type of gravitational perturbations.

The equation of motion for gravitational perturbations of scalar type can be reduced to the wavelike equation [3],

$$\left(\frac{d^2}{dr_*^2} + \omega^2 - V_\pm\right)\Psi(r) = 0, \tag{5}$$

where *the tortoise coordinate* r_* is defined as

$$dr_* = \frac{dr}{f(r)}, \tag{6}$$

$$V_\pm(r) = f(r)\frac{U_\pm}{64 r^2 H_\pm^2}. \tag{7}$$

Here V_+ and V_- are potentials for the two kinds of scalar gravitational perturbations. The potential V_- reduces to the pure gravitational perturbations when the black hole charge vanishes, while V_+ reduces to the perturbations of the test Maxwell field in the black hole background in this limit. When the charge Q is nonzero, the gravitational and electromagnetic perturbations are coupled.

Note that V_+ is proven to be stable [2] with the help of the S-deformation. Thus we are left with the V_- potential, which must be tested on stability.

Here we used the values

$$H_- = \lambda + \frac{d(d+1)}{2}(1 + \lambda\delta)X, \tag{8}$$

$$U_- = [-4d^3(d+2)(d+1)^2(1+\lambda\delta)^2X^2 + 48d^2(d+1)(d-2)\lambda(1+\lambda\delta)X - 16(d-2)(d-4)\lambda^2]Y - d^3(3d-2)(d+1)^4\delta(1+\lambda\delta)^3X^4 - 4d^2(d+1)^2(1+\lambda\delta)^2\{(d+1)(3d-2)\lambda\delta - d^2\}X^3 + 4(d+1)(1+\lambda\delta)\{\lambda(d-2)(d-4)(d+1)(\lambda+d^2)\delta + 4d(2d^2-3d+4)\lambda + d^2(d-2)(d-4)(d+1)\}X^2 - 16\lambda\{(d+1)\lambda(-4\lambda + 3d^2(d-2))\delta + 3d(d-4)\lambda + 3d^2(d+1)(d-2)\}X + 64\lambda^3 + 16d(d+2)\lambda^2. \quad (9)$$

We shall imply that

$$\Psi \sim e^{-i\omega t}, \qquad \omega = \omega_{\mathrm{Re}} - i\omega_{\mathrm{Im}},$$

so that $\omega_{\mathrm{Im}} > 0$ corresponds to a stable (decayed) mode, while $\omega_{\mathrm{Im}} < 0$ corresponds to an unstable (growing) mode. If the effective potential $V(r)$ is positive definite everywhere outside the black hole event horizon, the differential operator

$$\frac{d^2}{dr_*^2} + \omega^2$$

is a positive self-adjoint operator in the Hilbert space of the square integrable functions of r^*, and, in that case any solution of the wave equation with compact support is bounded, which implies stability. An important feature of the gravitational perturbations is that the effective potential V_- [Eq. (7)], which governs the scalar type of the perturbations, has negative gap for the higher dimensional black holes. Therefore the instability is not excluded for this case, and numerical analysis of perturbations is necessary.

The values

$$2\lambda\delta = \sqrt{1 + \frac{4\lambda Q^2}{(d+1)^2M^2}} - 1, \qquad \lambda = (\ell+d)(\ell-1), \qquad \ell = 2, 3, 4\ldots$$

are constants.

For convenience we shall parametrize the black hole mass and charge by its event horizon r_+ and inner horizon $r_- < r_+$, respectively. The value $r_- = 0$ corresponds to the uncharged black hole.

III. NUMERICAL METHOD

For analysis of stability, we need to test a black hole response to external perturbations, which is dominated by the so-called quasinormal modes at late time. The quasinormal boundary conditions correspond to the pure outgoing waves at infinity and pure incoming waves at the event (or de Sitter) horizon for asymptotically flat or de Sitter black holes. For asymptotically AdS black holes, the Dirichlet boundary conditions are imposed at infinity. If growing modes exist, the considered system is unstable. Although usually, damped quasinormal modes have both real and imaginary parts, i.e. are oscillating, the growing modes [8] are *nonoscillating*, that is *pure imaginary*. This makes our search of unstable modes much easier.

Below we shall discuss the numerical method, which we used here for asymptotically anti-de Sitter space-times.

Let us start from the analysis of singularities of the equation (5). At the event horizon $V_\pm(r) \propto f(r) \sim 0$. Therefore

$$\Psi(r) \sim (r - r_+)^{\pm i\omega/f'(r_+)}.$$

The quasinormal boundary conditions at the event horizon imply

$$\Psi(r) = (r - r_+)^{-i\omega/f'(r_+)}(Z_0 + \mathcal{O}(r - r_+)).$$

At the spatial infinity the two linear independent solutions of $\Psi(r)$ are

$$\Psi_1(r) \sim r^{-(D-4)/2}, \qquad \Psi_2(r) \sim r^{(D-6)/2}, \qquad D \neq 5,$$
$$\Psi_1(r) \sim r^{-1/2}, \qquad \Psi_2(r) \sim r^{-1/2}\ln(r), \qquad D = 5. \quad (10)$$

The quasinormal boundary conditions imply that

$$\Psi(r \to \infty) \propto \begin{cases} r^{-1}, & D = 4; \\ r^{-1/2}, & D = 5; \\ r^{-(D-4)/2}, & D \geq 6. \end{cases} \quad (11)$$

Let us consider the new function

$$y(r) = \left(\frac{r - r_+}{r - r_-}\right)^{i\omega/f'(r_+)}\Psi(r). \quad (12)$$

If $\Psi(r)$ satisfies the quasinormal boundary conditions, $y(r)$ is regular at the event horizon. Since the function $y(r)$ satisfies the linear equation, we fix its scale as

$$y(r_+) = 1.$$

Then $y'(r_+)$ can be found from the equation (5),

$$y'(r_+) = \frac{i\omega f''(r_+)}{2f'(r_+)^2} - \frac{i\omega}{(r_+ - r_-)f'(r_+)} + \frac{V_0}{f'(r_+) - 2i\omega},$$

where

$$V_0 = \lim_{r\to r_+}\frac{V_\pm(r)}{f(r)} = \frac{U_\pm(r_+)}{64r_+^2H_\pm^2(r_+)}.$$

Imposing the above discussed boundary conditions at the event horizon, we solve the equation (5) numerically for each ω using the NDSolve built-in function in MATHEMATICA for $r \geq r_f$, where $r_f \gg r_+$.

In the general case the behavior of $\Psi(r)$ at infinity is a superposition of the two solutions (10)

$$\Psi_f(r) = Z_i \Phi_i(r) + Z_d \Phi_d(r), \tag{13}$$

where $\Psi_d(r)$ satisfies the quasinormal boundary condition (11). If ω is the quasinormal frequency, the corresponding solution must satisfy the boundary conditions (11) at the spatial infinity and, thereby, $Z_i = 0$.

Thus, our numerical procedure is the following. We integrate the equation (5) numerically imposing a quasinormal boundary condition at the event horizon. At large distances we compare the obtained function $\Psi(r_f)$ with (13) and find, thereby, the coefficients Z_i and Z_d for any given value of ω. The quasinormal modes correspond to the roots of the equation

$$Z_i(\omega) = 0. \tag{14}$$

In order to find Z_i and Z_d, one has to find analytically expansions of $\Phi_i(r)$ and $\Phi_d(r)$ at large distances. The expansion

$$\Phi_d = \left\{ \begin{array}{ll} r^{-1}, & D = 4 \\ r^{-(D-4/2)}, & D \geq 5 \end{array} \right\} \left(1 + \frac{C_1^{(d)}}{r} + \frac{C_2^{(d)}}{r^2} + \frac{C_3^{(d)}}{r^3} \cdots \right) \tag{15}$$

contains only inverse powers of r, while the expansion

$$\Phi_i = \left\{ \begin{array}{ll} 1, & D = 4 \\ r^{-1/2} \ln(r), & D = 5 \\ r^{(D-6/2)}, & D \geq 6 \end{array} \right\} \left(1 + \frac{C_1^{(i)}}{r} + o\left(\frac{1}{r}\right)\right) \tag{16}$$

contains also subdominant terms of the form of order $\frac{\ln(r)}{r}$. Since the series in (16) are convergent we have used only the first term of the expansion, which does not contain a logarithm. The expansion of (15) was done up to the order $\sim r^{-3}$.

The analytical expansion allows one to find $\Phi_i(r)$ and $\Phi_d(r)$ within the desired precision for $r \gg r_+$. If $\Psi(r_f)$ were known exactly, one would had found the coefficients Z_i and Z_d from the system of the linear equations,

$$\Psi(r_f) = \Psi_f(r_f), \tag{17}$$

$$\Psi'(r_f) = \Psi'_f(r_f). \tag{18}$$

In practice, being the result of the numerical integration, the values $\Psi(r_f)$ and $\Psi'(r_f)$ contain a numerical error, which causes low precision of the coefficients Z_i and Z_d, found in this way. In order to minimize the numerical error, we find numerically the values of Ψ at some large number of points near $r = r_f$. Then we fit the obtained numerical values of Ψ by the function $\Psi_f(r)$ (13). From the fit data we find Z_i and Z_d by solving the least squares problem at those points.

Since unstable modes are purely imaginary, one can restrict the searching area for ω by the imaginary axis. In this case the problem simplifies because the eigenfrequencies and the coefficients Z_i, Z_d are real. It turns out that the coefficient Z_i changes its sign when crossing the solution. This can be used as an indicator of the existence of an unstable mode in the spectrum.

In order to be sure that the above method indeed can find an instability, we tested it for the two cases when the instability is determined both analytically and numerically by an alternative method. Namely, we checked the instability of the black strings [7,8], and also found the unstable modes of the Gauss-Bonnet black hole. Their values are in agreement with those obtained within time-domain integration. Thus, as an example, on Fig. 2 one can see that the unstable mode is $\omega = 0.18i$, which perfectly agrees with the value of unstable mode, obtained by the time-domain integration method in [10].

Another restriction upon the possible values of unstable modes comes from the depth of the negative potential gap ($V - \omega^2 > 0$ guarantees stability),

$$\mathrm{Im}\,(\omega) < \sqrt{-V_{\min}},$$

where $V_{\min}$ is the minimal value of the effective potential at $r_+ \leq r < \infty$.

For complex quasinormal frequencies Z_i is complex. For this case the solution of (14) can be found by minimizing $|Z_i(\omega)|$. Unfortunately, due to oscillation of the solution in the asymptotically flat and asymptotically de Sitter backgrounds, we were unable to fit the solution at very large distances. However, for asymptotically AdS background the solution does not oscillate at large distances, and the described approach can be used to find quasinormal modes of stable solutions.

IV. STABILITY ANALYSIS

For testing the stability, we have to perform two tasks: to check that the there is no unstable modes by the method described in the previous section for the full range of the black hole parameters and, as a confirmation, to find the fundamental (damped, when the system is stable) quasinormal modes.

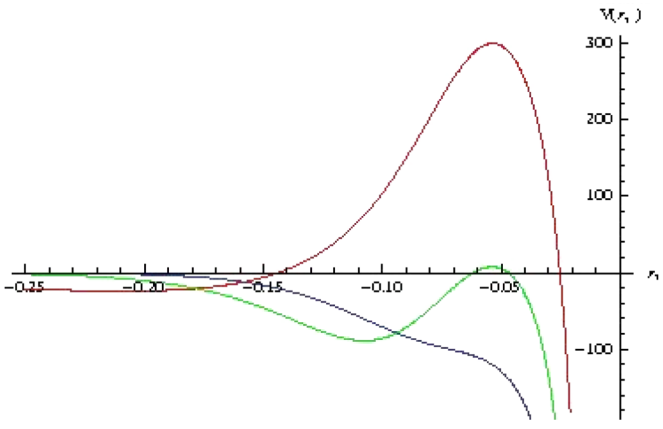

FIG. 1 (color online). Effective potential for the scalar type of gravitational perturbations of the RNAdS black holes for $D = 5$, $r_+ = 10R$.

We shall distinguish here three regimes: large black holes $r_+ \gg R$, intermediate black holes $r_+ \sim R$, and small black holes $r_+ \ll R$, where R is the anti-de Sitter radius. From Figs. 1–16, we can see that, for the $D = 5, 6 \ldots 11$ black holes, Z_i does not equal zero for any values of ω limited by $\mathrm{Im}(\omega) < \sqrt{-V_{\min}}$. We have shown this here mainly for the two values of r_+: $r_+ = 1R$ and $r_+ = 6R$. These are representative cases of large and intermediate AdS black holes. For small black holes, an example of Z_i behavior can be seen in Fig. 17 for $D = 5$. There one can see that the smaller the size of the black hole, the larger Z_i, which guarantees no instability at a sufficiently small black

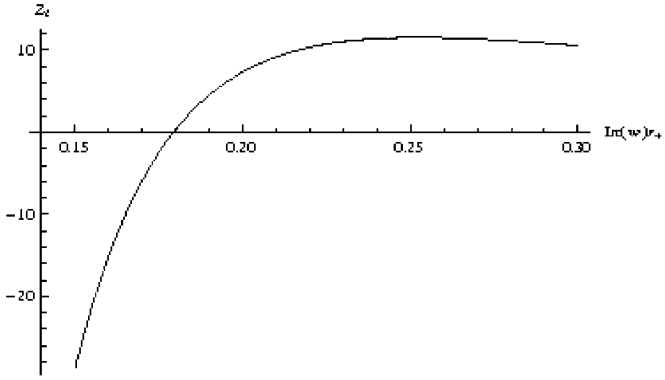

FIG. 2. Sample of instability for the Gauss-Bonnet black holes, $D = 5$, $\ell = 2$, $\alpha = 0.5$. Instability corresponds to zero of Z_i.

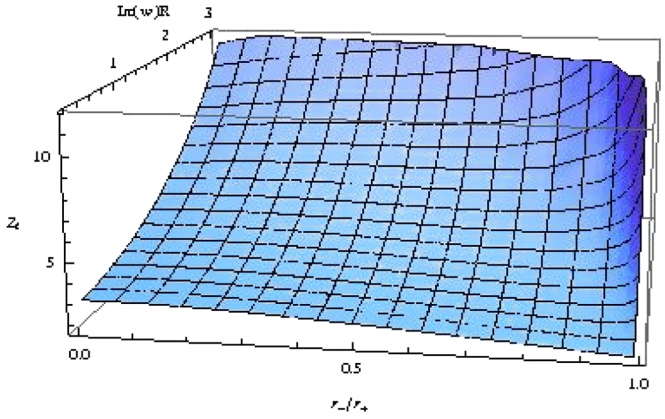

FIG. 3 (color online). Z_i as a function of r_-/r_+ and $\mathrm{Im}(\omega)R$ for $D = 5$, $r_+ = R$.

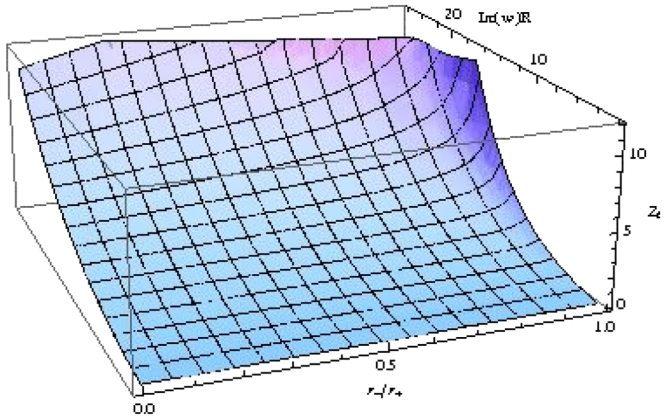

FIG. 4 (color online). Z_i as a function of r_-/r_+ and $\mathrm{Im}(\omega)R$ for $D = 5$, $r_+ = 10R$.

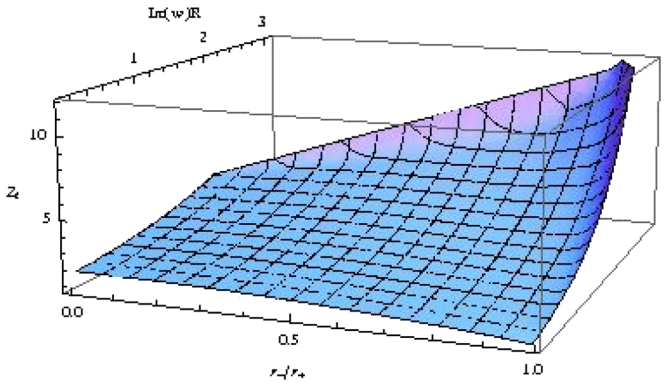

FIG. 5 (color online). Z_i as a function of r_-/r_+ and $\mathrm{Im}(\omega)R$ for $D = 6$, $r_+ = R$.

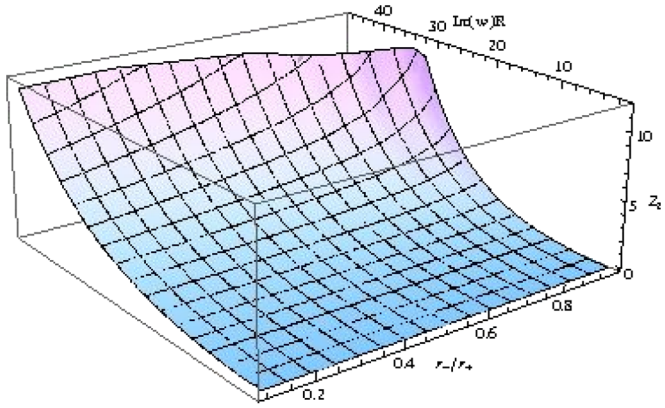

FIG. 6 (color online). Z_i as a function of r_-/r_+ and $\mathrm{Im}(\omega)R$ for $D = 6$, $r_+ = 10R$.

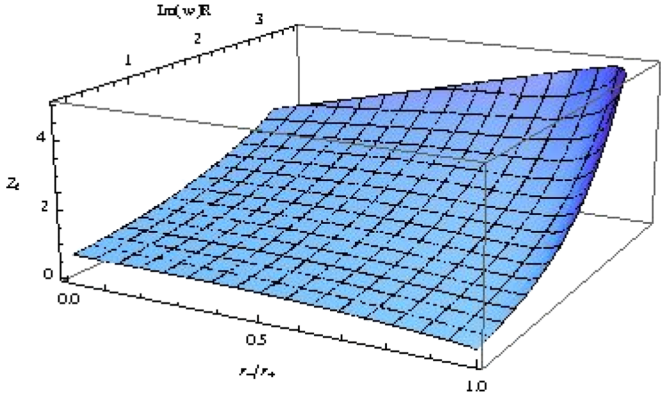

FIG. 7 (color online). Z_i as a function of r_-/r_+ and $\mathrm{Im}(\omega)R$ for $D = 7$, $r_+ = R$.

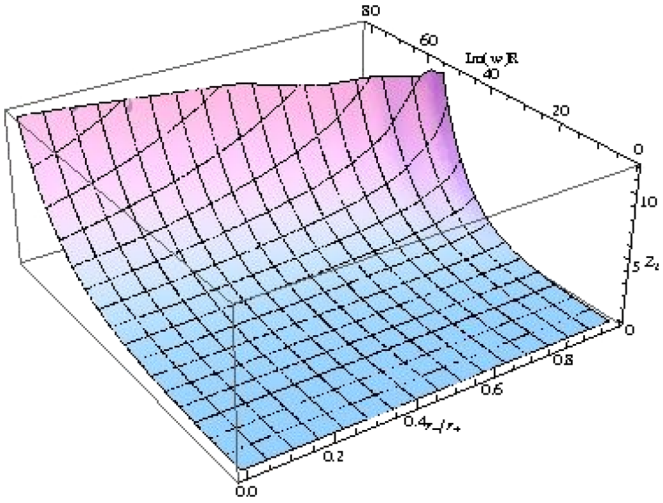

FIG. 8 (color online). Z_i as a function of r_-/r_+ and $\mathrm{Im}(\omega)R$ for $D = 7$, $r_+ = 10R$.

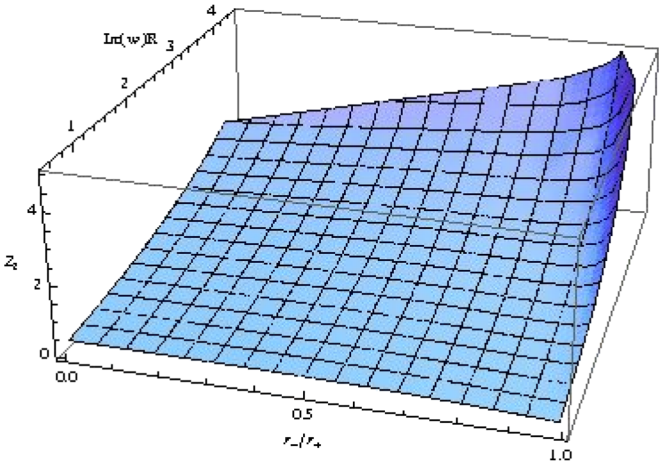

FIG. 9 (color online). Z_i as a function of r_-/r_+ and $\mathrm{Im}(\omega)R$ for $D = 8$, $r_+ = R$.

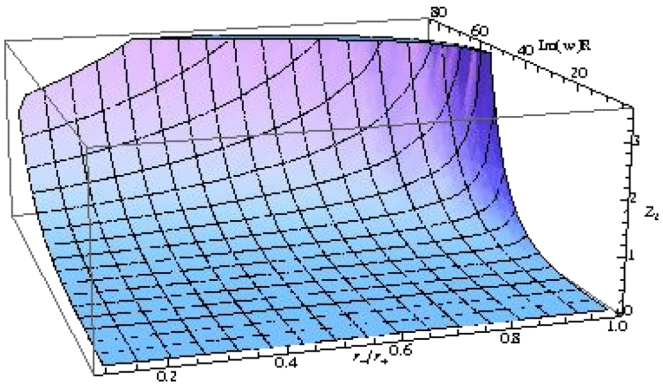

FIG. 10 (color online). Z_i as a function of r_-/r_+ and $\mathrm{Im}(\omega)R$ for $D = 8$, $r_+ = 10R$.

hole size. Looking carefully at all range of parameters of r_+, r_-, and ℓ, we have not found any zeros of Z_i. Therefore we conclude that $D = 5, 6 \ldots 11$ Reissner-Nordström-anti-de Sitter black holes are stable for any values of the black hole parameters. Now, we shall check this by the search of the fundamental quasinormal modes, which, as will be shown soon, all are damped.

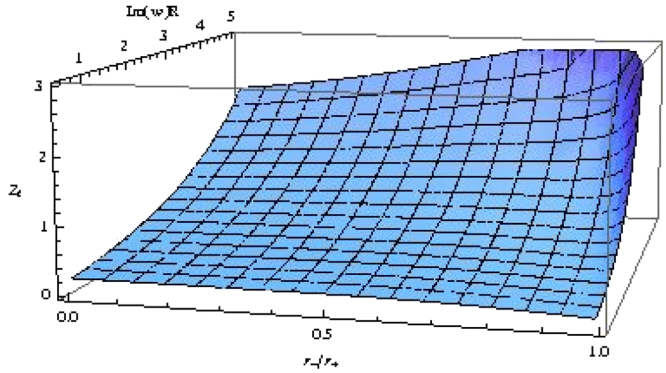

FIG. 11 (color online). Z_i as a function of r_-/r_+ and $\mathrm{Im}(\omega)R$ for $D = 9$, $r_+ = R$.

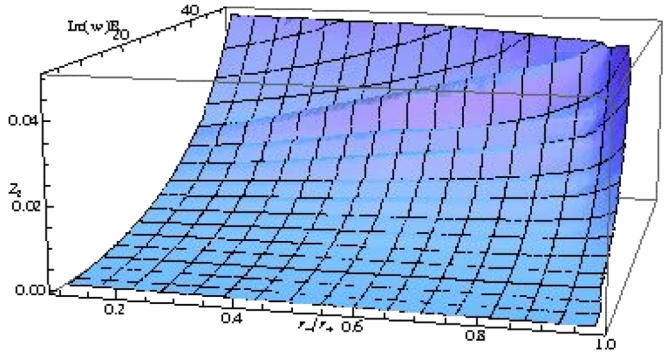

FIG. 12 (color online). Z_i as a function of r_-/r_+ and $\mathrm{Im}(\omega)R$ for $D = 9$, $r_+ = 10R$.

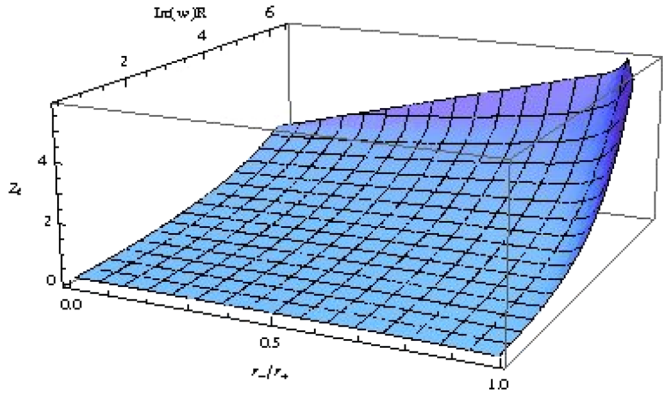

FIG. 13 (color online). Z_i as a function of r_-/r_+ and $\mathrm{Im}(\omega)R$ for $D = 10$, $r_+ = R$; logarithmic plot.

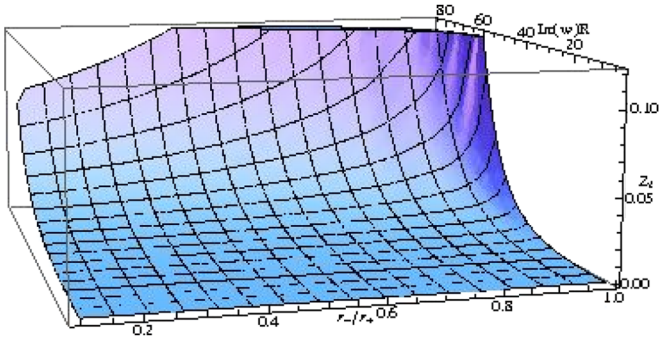

FIG. 14 (color online). Z_i as a function of r_-/r_+ and $\mathrm{Im}(\omega)R$ for $D = 10$, $r_+ = 10R$; logarithmic plot.

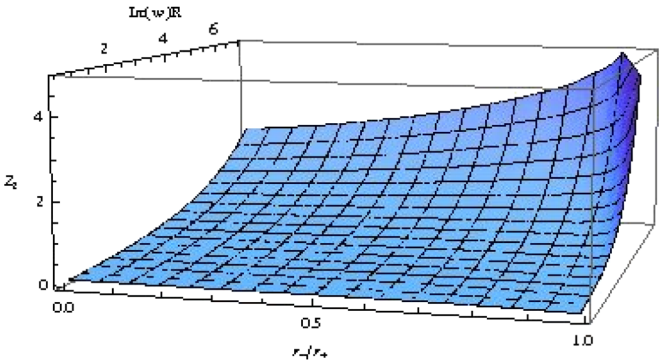

FIG. 15 (color online). Z_i as a function of r_-/r_+ and $\mathrm{Im}(\omega)R$ for $D = 11$, $r_+ = R$.

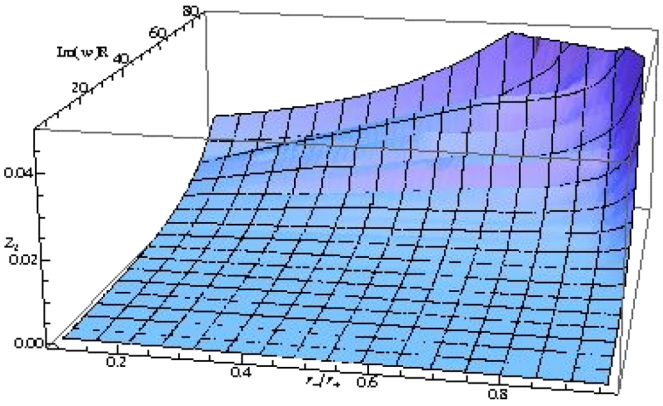

FIG. 16 (color online). Z_i as a function of r_-/r_+ and $\mathrm{Im}(\omega)R$ for $D = 11$, $r_+ = 10R$

The spectrum of frequencies of neutral asymptotically AdS black holes is qualitatively different from asymptotically flat or de Sitter cases: the main striking feature of the spectrum is that almost all modes are proportional to the radius of the black holes for large black holes $r_+ \gg R$. The exception is the fundamental mode of the scalar type of gravitational perturbations of Schwarzschild-anti-de Sitter (SAdS) black holes: its real part approaches constant as r_+ goes to infinity, while the imaginary part is inverse proportional to the radius of the black hole. Let us note that this property keeps also when AdS black holes are charged.

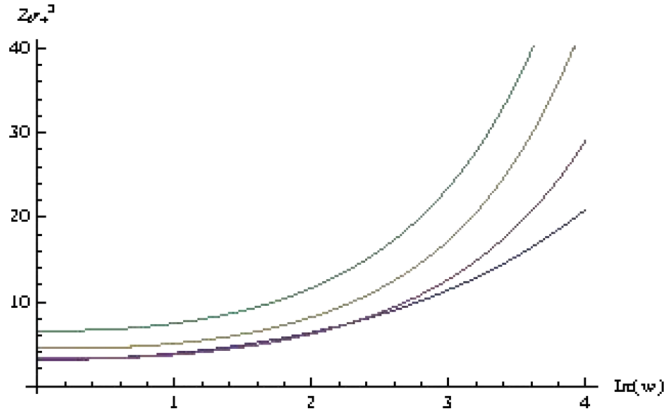

FIG. 17 (color online). Z_i for small Schwarzschild-AdS black holes $D = 5$; blue (top) for $r_+ = R$, red for $r_+ = R/2$, yellow for $r_+ = R/4$, green (bottom) for $r_+ = R/8$.

Quasinormal modes of a particular case of large $D = 5$ SAdS were considered in [19]. One can see in Table I that we accurately reproduce their results. The fundamental quasinormal modes for large Reissner-Nordstrom-anti-de Sitter black holes for $D = 6, 7$ can be seen in Table II. Indeed, the $Q = 0$, $r_+ = 6$ mode in Table I coincides with the fundamental mode of [19] in proper units (see Table III in [19]).

Another property of asymptotically AdS black holes is that their quasinormal modes approach the real normal modes of the pure anti-de Sitter black holes, when the radius of the black hole goes to zero [20]. This was shown for the test scalar field perturbations around $D = 5$ and 6 SAdS black holes in [20]. Here we have shown that, for the scalar type of gravitational perturbations, quasinormal modes also reach their $D \geq 6$ pure anti-de Sitter values

$$\omega_n R = 2n + D + \ell - 3, \qquad D \geq 6 \text{ pure AdS}. \quad (19)$$

The above formula for AdS space-time normal modes ω_n

TABLE I. Fundamental ($n = 0$) quasinormal modes of $D = 5$ Reissner-Nordström-AdS black holes.

r_-/r_+	$D = 5$, $r_+ = 1$	$D = 5$, $r_+ = 6$
0	2.204 77 − 0.581 37 i	1.651 71 − 0.137 59 i
0.1	2.196 46 − 0.577 76 i	1.651 43 − 0.136 23 i
0.2	2.172 55 − 0.567 54 i	1.650 58 − 0.132 14 i
0.3	2.135 71 − 0.552 36 i	1.649 14 − 0.125 44 i
0.4	2.089 34 − 0.534 45 i	1.647 13 − 0.116 39 i
0.5	2.036 98 − 0.516 37 i	1.644 55 − 0.105 49 i
0.6	1.982 48 − 0.500 74 i	1.641 50 − 0.093 50 i
0.7	1.930 93 − 0.489 56 i	1.638 00 − 0.081 31 i
0.8	1.888 85 − 0.480 91 i	1.634 04 − 0.069 89 i
0.9	1.856 19 − 0.468 02 i	1.629 44 − 0.060 59 i
0.99	1.899 19 − 0.246 19 i	1.626 48 − 0.056 44 i

TABLE II. Fundamental ($n = 0$) quasinormal modes of $D = 6, 7$ Reissner-Nordström-AdS black holes.

r_-/r_+	$D = 6$, $r_+ = 6$	$D = 7$, $r_+ = 6$
0	1.597 84 − 0.149 33 i	1.564 42 − 0.155 17 i
0.1	1.597 81 − 0.149 18 i	1.564 42 − 0.155 15 i
0.2	1.597 61 − 0.148 14 i	1.564 38 − 0.154 92 i
0.3	1.597 08 − 0.145 33 i	1.564 20 − 0.153 92 i
0.4	1.596 03 − 0.139 94 i	1.563 72 − 0.151 23 i
0.5	1.594 30 − 0.131 38 i	1.562 70 − 0.145 67 i
0.6	1.591 75 − 0.119 54 i	1.560 86 − 0.136 07 i
0.7	1.588 32 − 0.105 03 i	1.557 90 − 0.121 80 i
0.8	1.583 95 − 0.089 23 i	1.553 59 − 0.103 64 i
0.9	1.578 29 − 0.074 27 i	1.547 53 − 0.084 09 i
0.99	1.572 67 − 0.066 64 i	1.539 68 − 0.072 00 i

[21] is valid only for $D > 5$, while for $D = 5$ the pure AdS spectrum is continuous, i.e. all modes are normal modes of $D = 5$ AdS space-time. This happens because of the peculiar behavior of the effective potential at spatial infinity (which is zero in the tortoise coordinate): the effective potential has infinite negative pitch near $r^* = 0$ (see Fig. 1), so that $\Psi \to 0$ for all ω [21]. Notice that, in spite of the infinite negative pitch, the area covered by the pitch is finite, so that the instability is not guaranteed *a priori* even for this case. The natural question arises: does the limit of small black holes have the same meaning for $D = 5$ as it has for $D \geq 6$? In Fig. 18 one can see that, in the limit of small black holes, the $D = 5$ quasinormal modes (QNMs) approach the same limit as $D \geq 6$ modes. The latter can be easily understood if we remember that we used the QNMs boundary conditions motivated by the AdS/CFT interpretation, i.e. we chose the specific falloff of the field at infinity, according to the formula (11), while the continuous spectrum of pure AdS space-time is obtained with the Dirichlet boundary conditions [21]. When choosing the AdS/CFT inspired falloff (11), the same discrete spectrum (19) is obtained for the $D = 5$ pure AdS space-time, so that QNMs of small AdS black holes approach their pure AdS values for all D.

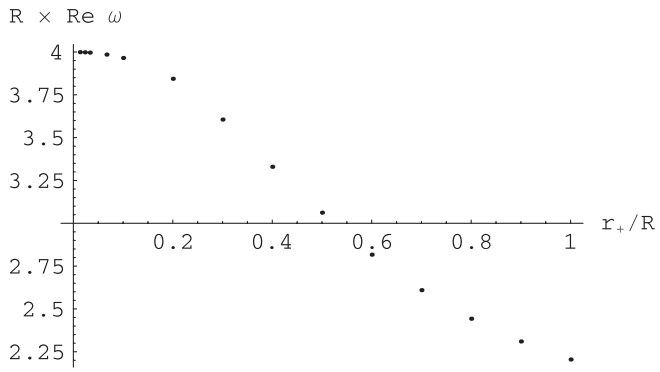

FIG. 18. Re $\omega_{n=0}$ for small $D = 5$ Schwarzschild-AdS black holes approaches the limit $\omega = 4$ as $r_+ \to 0$.

It is not remarkable that, for Reissner-Nordström-AdS black holes, QNMs approach the same pure AdS values in the limit $r_+ \to 0$ (19), because one cannot assume $r_+ = 0$, without taking $Q = 0$. Thus, the fundamental quasinormal modes of the scalar type of gravitational perturbations of D-dimensional RNAdS black holes obey

$$\omega_n R \to 2n + D + \ell - 3, \qquad r_+ \to 0, \qquad D \geq 5. \tag{20}$$

Let us note that, once we proved here the stability of the D-dimensional Schwarzschild-AdS black holes, the stability of the Reissner-Nordström-AdS black holes can be intuitively understood from the behavior of the effective potentials (figures for scalar type in [2,3]) at least for $D \geq 6$: the presence of the charge Q increases slightly the negative depth of the potential gap. Apparently the negative gap is not deep enough to allow bound states with negative "energy." The behavior of the effective potential for $D = 5$ is quite different (17), yet, as we have shown, this does not lead to instability as well.

V. DISCUSSIONS

In this paper, by the numerical search of quasinormal modes, we have shown that Reissner-Nordström-anti-de Sitter black holes are gravitationally stable in $D = 5, 6 \ldots 11$ space-time dimensions. Before, the stability of asymptotically anti-de Sitter black holes was established only for $D = 4$ Reissner-Nordström-anti-de Sitter black holes analytically [2]. Stability for $D = 5$–11 found here and for $D = 4$ found by Ishibashi and Kodama [2] does not contradict the observed instability for $D = 4, 5$ RNAdS black holes by Gubser and Mitra in [15,16], because the latter instability is induced by a tachyonic field coupled to the system in the $\mathcal{N} = 8$ gauged supergravity. Thus, although metrics for the black hole in both cases are the same RNAdS metric, they are an exact solution of different field equations, and the dynamic of perturbed equations is certainly different.

The stability of RNAdS black holes observed here is interesting also, because we know that small AdS black holes (within the ordinary Einstein-Maxwell theory, considered here) are thermodynamically unstable and may exert the Hawking-Page transition. It would be natural to expect that this thermodynamic transition will be accompanied by a gravitational instability. Yet, as we have shown here, this does not take place, so that if the correlation between thermodynamic and gravitational instabilities exists, it is more subtle than one could naively expect for complex gravitational systems.

An important question, which was beyond the scope of our work, is the stability of extremally charged RNAdS black holes. Our closest aim is to give detailed data on quasinormal modes of other types of gravitational perturbations (vector and tensor), and to find higher overtones of the spectrum [22]. We believe it would be interesting to

investigate stability of charged asymptotically AdS black holes in the Gauss-Bonnet theory, where already there is instability, stipulated by Gauss-Bonnet terms, at higher multipoles.

ACKNOWLEDGMENTS

We would like to acknowledge Andrei Starinets for very valuable discussions. R. K. acknowledges support of the Japan Society for the Promotion of Science (JSPS). A. Z. was supported by Fundação de Amparo à Pesquisa do Estado de São Paulo (FAPESP), Brazil.

[1] P. Horava and E. Witten, Nucl. Phys. **B460**, 506 (1996); N. Arkani-Hamed, S. Dimopoulos, and G. R. Dvali, Phys. Lett. B **429**, 263 (1998); L. Randall and R. Sundrum, Phys. Rev. Lett. **83**, 3370 (1999).

[2] H. Kodama and A. Ishibashi, Prog. Theor. Phys. **111**, 29 (2004).

[3] A. Ishibashi and H. Kodama, Prog. Theor. Phys. **110**, 901 (2003).

[4] R. A. Konoplya and A. Zhidenko, Nucl. Phys. **B777**, 182 (2007).

[5] M. Kimura, K. Murata, H. Ishihara, and J. Soda, Phys. Rev. D **77**, 064015 (2008).

[6] H. Ishihara, M. Kimura, R. A. Konoplya, K. Murata, J. Soda, and A. Zhidenko, Phys. Rev. D **77**, 084019 (2008).

[7] R. Gregory and R. Laflamme, Phys. Rev. Lett. **70**, 2837 (1993).

[8] R. A. Konoplya, K. Murata, J. Soda, and A. Zhidenko, Phys. Rev. D **78**, 084012 (2008).

[9] M. Beroiz, G. Dotti, and R. J. Gleiser, Phys. Rev. D **76**, 024012 (2007); R. J. Gleiser and G. Dotti, Phys. Rev. D **72**, 124002 (2005).

[10] R. A. Konoplya and A. Zhidenko, Phys. Rev. D **77**, 104004 (2008).

[11] P. Kanti, R. A. Konoplya, and A. Zhidenko, Phys. Rev. D **74**, 064008 (2006); P. Kanti and R. A. Konoplya, Phys. Rev. D **73**, 044002 (2006); S. K. Chakrabarti, arXiv:0809.1004; M. Nozawa and T. Kobayashi, Phys. Rev. D **78**, 064006 (2008); H. T. Cho, A. S. Cornell, J. Doukas, and W. Naylor, Phys. Rev. D **77**, 041502 (2008); R. A. Konoplya and E. Abdalla, Phys. Rev. D **71**, 084015 (2005); U. A. al-Binni and G. Siopsis, Phys. Rev. D **76**, 104031 (2007); R. Daghigh and M. Green, arXiv:0808.1596; A. Lopez-Ortega, Gen. Relativ. Gravit. **40**, 1379 (2008); E. Abdalla, C. B. M. Chirenti, and A. Saa, J. High Energy Phys. 10 (2007) 086; S. Chen, B. Wang, and R. K. Su, Phys. Lett. B **647**, 282 (2007); R. G. Daghigh, G. Kunstatter, D. Ostapchuk, and V. Bagnulo, Classical Quantum Gravity **23**, 5101 (2006); E. Abdalla, R. A. Konoplya, and C. Molina, Phys. Rev. D **72**, 084006 (2005); R. Konoplya, Phys. Rev. D **71**, 024038 (2005); R. A. Konoplya, Phys. Rev. D **68**, 024018 (2003); E. Berti, K. D. Kokkotas, and E. Papantonopoulos, Phys. Rev. D **68**, 064020 (2003); V. Cardoso, J. P. S. Lemos, and S. Yoshida, Phys. Rev. D **69**, 044004 (2004).

[12] R. A. Konoplya and A. Zhidenko, arXiv:0809.2822.

[13] E. Witten, Adv. Theor. Math. Phys.. **2**, 505 (1998).

[14] D. Birmingham, I. Sachs, and S. N. Solodukhin, Phys. Rev. Lett. **88**, 151301 (2002); V. Cardoso and J. P. S. Lemos, Phys. Rev. D **63**, 124015 (2001); P. Kovtun, D. T. Son, and A. O. Starinets, Phys. Rev. Lett. **94**, 111601 (2005); P. K. Kovtun and A. O. Starinets, Phys. Rev. D **72**, 086009 (2005); A. O. Starinets, arXiv:0806.3797; D. T. Son and A. O. Starinets, Annu. Rev. Nucl. Part. Sci. **57**, 95 (2007); V. Cardoso, R. Konoplya, and J. P. S. Lemos, Phys. Rev. D **68**, 044024 (2003); R. A. Konoplya, Phys. Rev. D **68**, 124017 (2003); I. Amado, C. Hoyos-Badajoz, K. Landsteiner, and S. Montero, arXiv:0805.2570; G. Siopsis, arXiv:0804.2713.

[15] S. S. Gubser and I. Mitra, arXiv:hep-th/0009126.

[16] S. S. Gubser and I. Mitra, J. High Energy Phys. 08 (2001) 018.

[17] S. W. Hawking and D. N. Page, Commun. Math. Phys. **87**, 577 (1983).

[18] A. Chamblin, R. Emparan, C. V. Johnson, and R. C. Myers, Phys. Rev. D **60**, 104026 (1999).

[19] J. J. Friess, S. S. Gubser, G. Michalogiorgakis, and S. S. Pufu, J. High Energy Phys. 04 (2007) 080.

[20] R. A. Konoplya, Phys. Rev. D **66**, 044009 (2002).

[21] J. Natario and R. Schiappa, Adv. Theor. Math. Phys. **8**, 1001 (2004).

[22] R. Konoplya, G. Siopsis, and A. Zhidenko (work in progress).